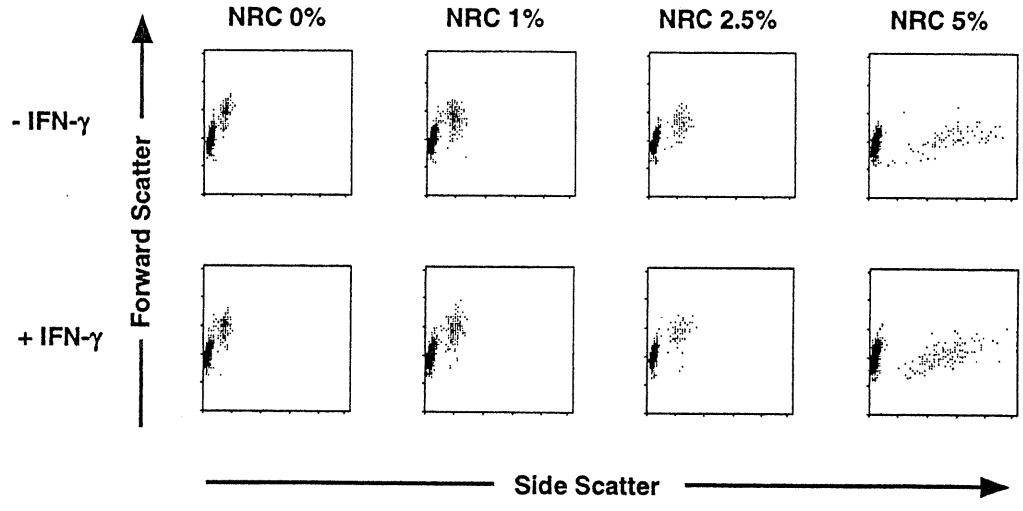

Figure 3: Analysis of forward/side scatter pattern of PBMCs cultured with various concentrations of NRC for 20 hr.

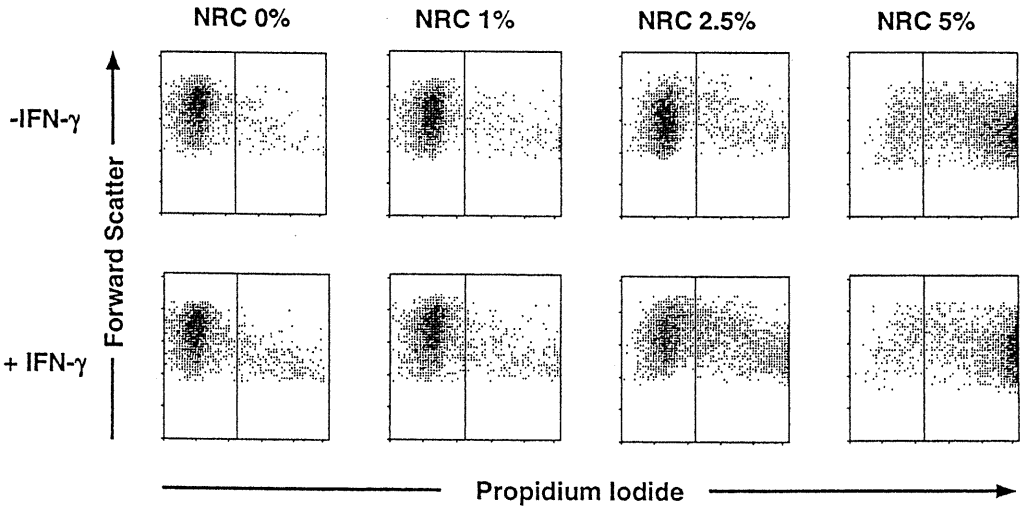

Figure 4: Representative propidium iodide (PI) staining pattern of monocytes cultured for 20 hr with various concentrations of NRC.

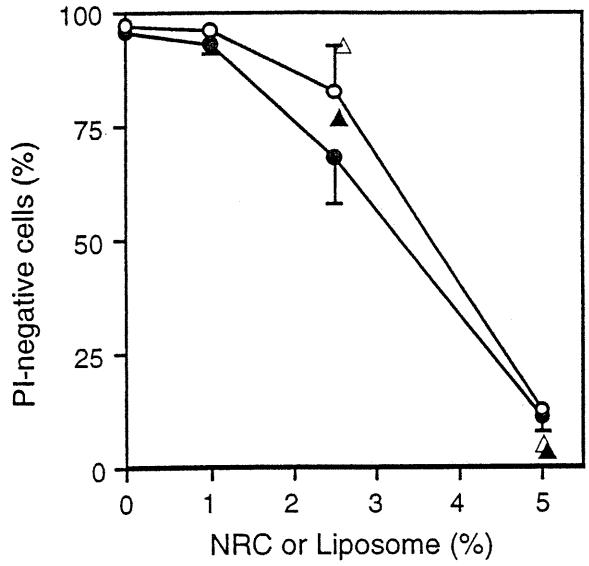

Figure 5: Effect of NRC (circles) or empty liposomes (triangles) on the viability of monocytes, as measured by PI negativity. PBMCs were treated for 20 hr with NRC at the concentrations indicated plus (closed) or minus (open) IFN-γ. The values are the mean ± SE from four donors.

Effect of NRC on the expression of costimulatory molecules on monocytes

The effect of NRC treatment on the expression of CD80 (B7-1), CD86 (B7-2), and CD54 (ICAM-1) on monocytes was also studied with a flow cytometric analysis (Fig. 6). PBMCs were exposed to NRC at concentrations up to 2.5%, where the reduction of monocyte viability was moderate. Resting monocytes show significant expressions of CD86 and CD54, but not CD80. A slight expression of CD80 on monocytes was induced by NRC treatment, whereas the constitutive expressions of CD86 and CD54 were unchanged. The activation of monocytes with IFN-γ induced the expressions of CD80, CD86, and CD54 under all conditions tested, but the IFN-γ-induced expressions of CD54 on monocytes tended to be less in the presence of NRC than those in the absence of NRC.

DISCUSSION

When macrophages and neutrophils ingest particles or are exposed to a variety of soluble stimuli, they markedly consume the oxygen reduced to superoxide anion (O_2^-) and converted to various reactive oxygen species including H_2O_2. In this study, we found that NRC or liposome treatment for up

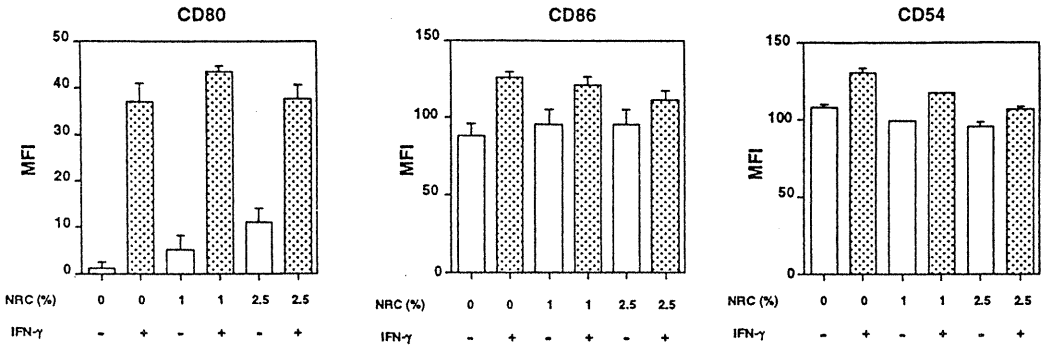

Figure 6: Effect of NRC on the expressions of CD80, CD86 and CD54 on monocytes in the presence or absence of IFN-γ. PBMCs were treated for 20 hr with NRC at the concentrations indicated. The net mean fluorescence intensity (MFI) was calculated by subtracting the MFI of control immunoglobulin-stained cells from the MFI of cells with test MoAb. The values are the mean ± SE from three donors.

to 150 min caused the potentiation of superoxide production by human monocytes in response to PMA. In contrast to the short incubation with NRC, the longer incubation caused the reduction of PMA-triggered superoxide production, which was associated with a reduction of monocyte viability. This effect was not specific to NRC, since the same effect was observed in the case of empty liposomes. Thus, hemoglobin itself in the liposome was not toxic to monocytes. The cell death of monocytes caused by NRC or liposome treatment was not apoptotic, but rather necrotic, as assessed by Annexin-V staining together with PI (data not shown).

Gonzalez-Rothi et al. showed no aberrent effects of liposomes, even at large concentrations, on the functions of rat plumonary macrophages including viability, phagocytic and killing activities, surface adherence, and respiratory burst (10). Moreover, several investigators studied the effects of LEH on cytokine productions by monocytes/macrophages (6-8). Although cytokine productions are affected by LEH, the viability appears to be unaffected. The disparity between the previous results and our present findings may be due to a number of parameters including the composition of the lipids, net amount of the lipids, the size of liposomes, the incubation period, and so on. Further study is needed to clarify these possibilities.

Costimulatory molecules including CD80, CD86 and CD54 are expressed on antigen-presenting cells such as monocytes and dendritic cells, and transduce costimulatory signals in interactions with counter-receptors on T

cells (11). We found that resting monocytes show significant expressions of CD86 and CD54, but not CD80 (12). Upon the activation of monocytes with various stimuli or the interaction with T cells, the expressions of these molecules are upregulated (12). Our preliminary efforts to define the effects of NRC on these costimulatory molecules showed that NRC treatment caused a slight induction of CD80. In contrast, the NRC treatment tended to decrease the IFN-• -induced expressions of CD54. Although the implications of these results regarding clinical significance require further study, our preliminary observations suggest that NRC administration may cause a reduction of monocyte viability as well as a modification of costimulatory signals, thereby affecting immunoresponses in patients.

ACKNOWLEDGMENTS

This work was partially supported by Health Science Research Grant (Artificial Blood Project) from the Ministry of Health and Welfare, Japan.

REFERENCES

1. M. Farmer, A. Rudolph, K. Vandergriff, M. Hayre, S. Bayne, and S, Johnson. Liposome encapsulated hemoglobin: oxygen binding properties and respiratory function. Biomater Artif Cells artif Organs 16:289-299, (1988).

2. A.S. Rudolph. Encapsulated hemoglobin: current issues and future goals. Art Cells Blood Subs Immob Biotech 22:347-360, (1994).

3. A. Usuba, R. Motoki, K. Suzuki, K. Sakaguchi, and A. Takahashi. Study of effect of the newly developed artificial blood 'Neo Red Cells (NRC)' on hemodynamics and blood gas transport in canine hemorrhagic shock. Biomater Artif Cells Immobil Biotechnol 20:531-535, (1992).

4. R. Rabinovici, A.S. Rudolph, J. Vernick, and G. Feuerstein. A new salutary resuscitative fluid: liposome encapsulated hemoglobin/hypertonic saline solution. J Trauma 35:121-126, (1993).

5. M. Takaori, and A. Fukui. Treatment of massive hemorrhage with liposome encapsulated human hemoglobin (NRC) and hydroxyethyl starch (HES) in beagles. Art Cells Blood Subs and Immob Biotech 24:643-653, (1996).

6. F.M. Rollwagen, W.C.M. Gafney, N.D. Pacheco, T.A. Davis, T.M.

Hickey, T.B. Nielsen and A.S. Rudolph. Multiple responses to administration of liposome-encapsulated hemoglobin (LEH): Effects on hematopoiesis and serum IL-6 levels. Exp Hematol 24:429-436, (1996).

7. L.A. Langdale, R.V. Maier, L. Wilson, T.H. Pohlman, J.G. Williams, C.L. Rice. Liposome-encapsulated hemoglobin inhibits tumor necrosis factor release from rabbit alveolar macrophages by a posttranscriptional mechanism. J Leukoc Biol 52:679-686, (1992).

8. A.S. Rudolph, R.O. Cliff, B.J. Spargo, and H. Spielberg. Transient changes in the mononuclear phagocyte system following administration of the blood substitute liposome-encapsulated haemoglobin. Biomaterials 15:796-804, (1994).

9. A.S. Rudolph, R.W. Klipper, B. Goins and W.T. Phillips. *In vitro* distribution of a radiolabelled blood substitute: ^{99m}Tc-liposome-encapsulated hemoglobin in an anesthetized rabbit. Proc Natl Acad Sci USA 88:10976-10980, (1991).

10. R.J. Gonzalez-Rothi, L. Straub, J.L. Cacace and H. Schreier. Liposomes and pulmonary alveolar macrophages: functional and morphologic interactions. Exp Lung Res 17:687-705, (1991).

11. E.C. Guinan, J.G. Gribben, V.A. Boussiotis, G.J. Freeman and L.M. Nadler. Pivotal role of the B7:CD28 pathway in transplantation tolerance and tumor immunity. Blood:3261-3282, 1994.

12. M. Fujihara, T.A. Takahashi, M. Azuma, C. Ogiso, T.L. Maekawa, H. Yagita, K. Okumura, and S. Sekiguchi. Decreased inducible expression of CD80 and CD86 in human monocytes after ultraviolet-B irradiation: its involvement in inactivation of allogenecity. Blood:2386-2393, 1996.

ART. CELLS, BLOOD SUBS., AND IMMOB. BIOTECH., 26(5&6), 559-570 (1998)

INFLAMMATORY CYTOKINE PRODUCTION IN WHOLE BLOOD MODIFIED BY LIPOSOME-ENCAPSULATED HEMOGLOBIN

Koichi Niwa, Kenji Ikebuchi, Mitsuhiro Fujihara, Hideki Abe, Shinobu Wakamoto, Takatoshi Ito, Miki Yamaguchi, and Sadayoshi Sekiguchi
Hokkaido Red Cross Blood Center, Sapporo 063, Japan

ABSTRACT

The effect of Neo Red Cells (NRC), liposome-encapsulated hemoglobin, on production of tumor necrosis factor alpha (TNF-α) and interleukin-6 (IL-6) were studied in whole blood preparations ex vivo. Venous blood was collected with heparin and incubated in a CO_2 incubator. Treatment of blood samples with NRC reduced the constitutive levels of TNF-α and IL-6. Lipopolysaccharide (LPS) treatment for 24 h increased production of TNF-α and IL-6 in a dose-dependent manner. Pretreatment with NRC (5%) for 24 h markedly potentiated the LPS-induced TNF-α production and, that of IL-6 to a lesser extent. Northern bloting analysis of total RNA in whole blood showed that pretreatment with NRC caused a marked increase in TNF-α mRNA expression in response to LPS. It is concluded that NRC potentiates LPS-induced TNF-α and IL-6 production in whole blood ex vivo, and that the potentiating effect of NRC on LPS-induced TNF-α production can be attributed, at least in part, to an increase in its mRNA expression.

INTRODUCTION

A large number of studies have been carried out for development and research of red cell substitutes [1]. The establishment of a red cell substitute may reduce some problems in transfusion such as risk of viral infection, requirement of blood typing and short shelf-life.

Liposome-encapsulated hemoglobin (LEH) is a potential red cell substitute. Many studies have been performed to evaluate the effects of LEH on several organs and biological responses [2]. Studies have revealed that LEH is ingested in reticuloendothelial systems [3] and modifies production of inflammatory cytokines such as tumor necrosis factor-α (TNF–α) and interleukin-6 (IL-6) [4-8]. Evaluation of the influence of LEH or liposomes on cytokine production has been performed with several in vivo and in vitro preparations; e.g. rat [6], mouse [7, 8], rabbit alveolar macrophages [4], human monocytes [5], and rat Kupffer's cells [6]. Due to the variety of experimental procedures, the modifications of cytokine production by LEH or liposomes have not been determined, although such information have gradually accumulated. Furthermore, clinical studies of LEH administration have not yet been carried out.

Over the last several years, whole blood preparations have been introduced for evaluation of blood cell functions including cytokine production [10,11]. Whole blood preparation is simple, and evaluation with such preparations is likely to mimic the clinical situation because the net effect of LEH, which may interact with not only blood cells but also serum elements [12], can be observed. We examined the effects of LEH on cytokine production with human whole blood samples to obtain further insight into the biocompartibility of LEH.

MATERIALS AND METHODS

LEH and liposome

Neo Red Cells (NRC), LEH suspended in saline solution, were kindly provided by Terumo Co. (Kanagawa, Japan); Human stroma-free hemoglobin was encapsulated in lipid vesicles composed of a 7:7:2:0.28 ratio of soybean hydrogenated phosphatidylcholine, cholesterol, myristic acid, and α-tocopherol. NRC were approximately 250 nm in diameter. Liposomes were also provided by Terumo Co. The composition of liposomes was the same as that of NRC except they did not contain human stroma-free hemoglobin. Superficial modification of both NRC and empty liposomes was carried out using polyethleneglycol-conjugated phosphatidylethanolamine to prevent agglutination.

Whole blood preparation

Blood was collected from healthy volunteers aged between 20-30 years old. Venous blood was collected into a bag containing heparin, the final

concentration of which was 170 U/mL. Collected blood was divided into three experimental groups: control, NRC, and liposome groups. Blood samples of control, NRC and liposome groups were supplemented with saline, NRC and liposomes, respectively, to a final concentration of 5% (V/V). Four-mL blood samples were added to each well of 6-well plates and placed in a CO_2 incubator with or without lipopolysaccharide (LPS; *E. coli* 0111:B4, Sigma Chemical Co., MO, USA).

Cytokine measurement

After incubation for appropriate periods, cultured blood samples were centrifuged, then the supernatant was collected. The levels of TNF-α and IL-6 proteins in the supernatants were determined in duplicate using cytokine-specific enzyme-immunosorbent immunoassay (ELISA) kits (R&D Systems, MN, USA) according to the manufacturer's recommendations.

Northern bloting analysis

After incubation for appropriate periods, total RNA was isolated from whole blood using a commercial kit (RNeasy Blood Mini Kits, QIAGEN Inc., CA, USA) according to the manufacturer's instructions. Equivalent amounts of RNA (4 μg) were size-fractionated by electrophoresis in 1% agarose gels containing 2.2 M formaldehyde. The RNA was then blotted onto Nytran membranes (S&S, Dassel, Germany). Human TNF-α cDNA fragments were obtained by reverse-transcription PCR from total RNA extracted from LPS-stimulated monocytes. The TNF-α fragment was cloned into pBluescript II (Stratagene Cloning Systems, La Jolla, CA). The linearlized plasmids containing the properly oriented insert were transcribed using an in vitro transcription kit (Ambion Inc., Austin, TX) with ^{32}P-UTP, and used for hybridization.

RESULTS

To investigate the effects of NRC on constitutive cytokine production, blood samples were treated with 5 % saline or NRC for 8 or 24 h. As shown in Fig. 1A, NRC caused a reduction in TNF-α production. Similarly, a reduction in IL-6 production by NRC was observed (Fig. 1B).

To mimic the clinical situation with bacterial infection, we added LPS to blood samples and examined the effects of NRC on the LPS-induced cytokine production. Fig. 2 shows dose-response curves of LPS-induced cytokine production. As expected, LPS treatment increased TNF-α production in a dose-dependent manner; at 8 and 24 h NRC slightly and

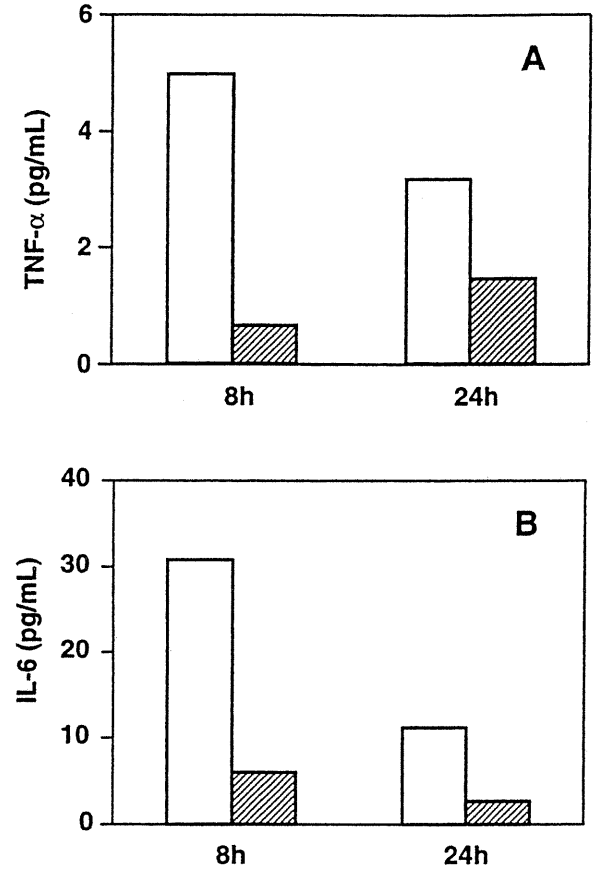

Fig.1 Effects of NRC on constitutive production of TNF-α (A) and IL-6 (B). Whole blood samples were incubated with 5% saline (open bar) or NRC (hatched bar) for 8 or 24 h. Similar results were obtained in another two experiments.

markedly potentiated TNF-α production, respectively (Fig. 2A). The potentiation by NRC was evident when samples were exposed to higher concentrations of LPS (Fig. 2A, right panel). LPS treatment increased IL-6 production dose-dependently (Fig. 2B). NRC also potentiated IL-6 production although its effect was weak (Fig. 2B, right panel).

We then investigated the time course of changes in LPS-induced cytokine production and examined the effect of NRC by two protocols: concurrent treatment with LPS and NRC, and pretreatment with NRC for 24 h followed by LPS treatment. When blood samples were stimulated with

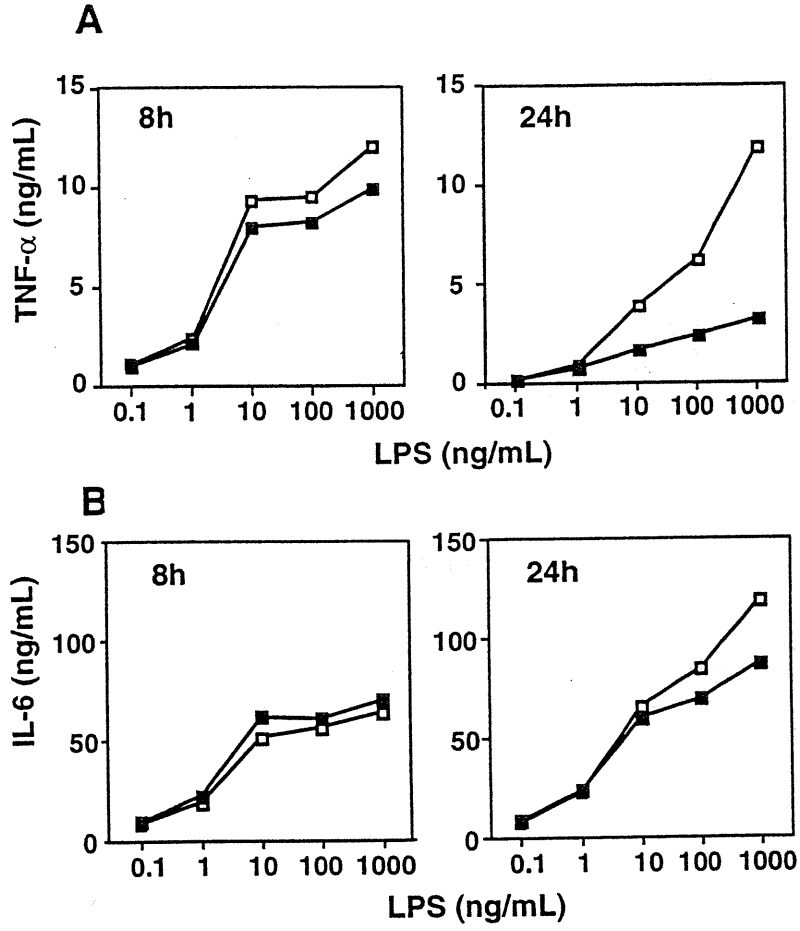

Fig.2 Effects of NRC on LPS-induced productions of TNF-α (A) and IL-6 (B). Whole blood samples containing 5% saline (open bar) or NRC (hatched bar) were incubated with several concentrations of LPS for 8 or 24 h. Similar results were obtained in other two experiments.

LPS, TNF-α production increased and reached a peak level at around 8 h, then decreased thereafter (Fig. 3A, left panel). Concurrent treatment with NRC potentiated the LPS-induced TNF-α level. TNF-α response to LPS was attenuated after 24 h of incubation without NRC, while pretreatment with NRC maintained a prominent TNF-α response to LPS (Fig. 3A, right panel). LPS treatment caused a gradual increase in IL-6 production in both protocols (Fig. 3B). In both protocols, NRC treatment slightly potentiated the IL-6 response to LPS, although the extent of potentiation was much lower than that of TNF-α.

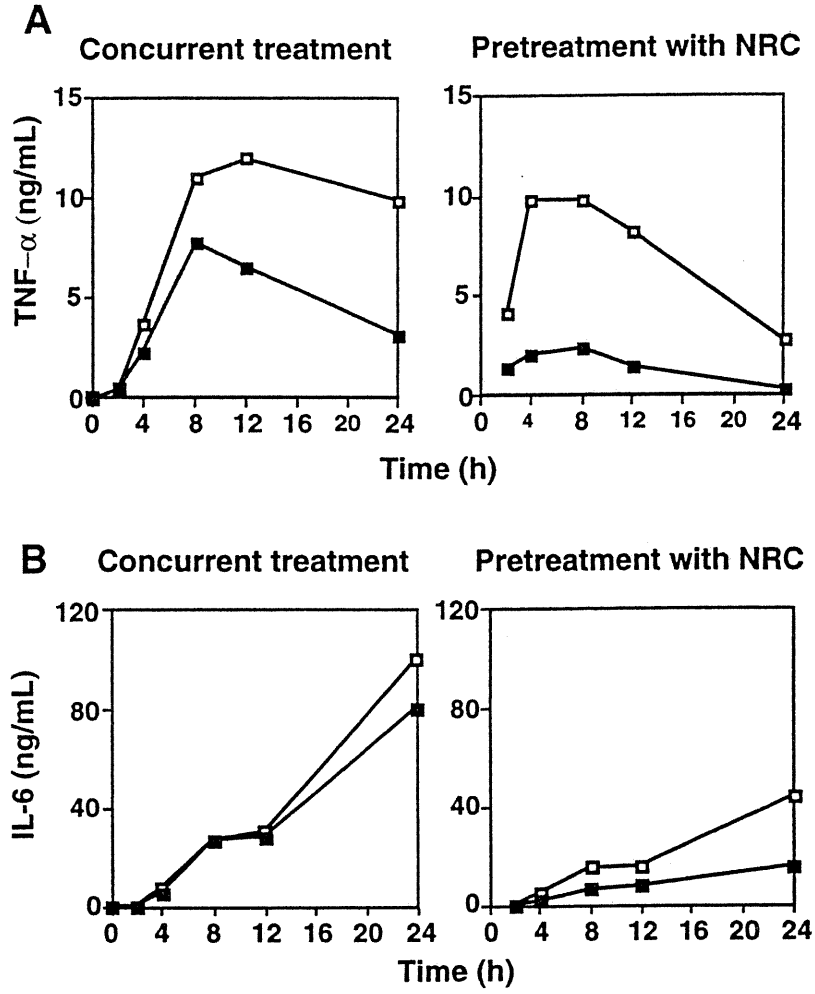

Fig.3 Effects of NRC on time course of changes in LPS-induced productions of TNF-α (A) and IL-6 (B). In the concurrent treatment protocol, whole blood samples containing 5% saline (closed squares) or NRC (open squares) were incubated with LPS (1 μg/mL) for 24 h. In the pretreatment protocol, whole blood samples were preincubated with 5% saline or NRC for 24 h and incubated with LPS for a further 24 h. Similar results were obtained in another two experiments.

We also examined the effects of liposomes which had the same lipid composition as NRC in whole blood samples, in comparison with NRC treatment. Whole blood was pretreated with NRC or liposome for 24 h and then treated with LPS for 24 h. Treatment with empty liposomes as well as NRC potentiated the LPS-induced TNF-α production (Fig. 4A). Similarly, pretreatment with liposomes potentiated LPS-induced IL-6 production (Fig. 4B). These results indicated that the potentiating effect of NRC on LPS-induced cytokine level is due, at least in part, to the liposomes themselves.

Pretreatment with NRC markedly potentiated LPS-induced TNF-α levels in whole blood samples. To determine whether the potentiating effect of NRC on TNF-α production is due to an increase in TNF-α mRNA level, we carried out northern bloting analysis. Blood samples were treated with NRC for 24 h and subsequently treated with LPS. Two and 4 h after LPS treatment, we extracted total RNA from blood samples and performed northern bloting analysis. At 2 h after LPS-treatment, TNF-α mRNA was expressed as shown in Fig. 5. Pre-treatment with NRC clearly potentiated TNF-α mRNA expression. Potentiation of the TNF-α mRNA level by NRC treatment was also observed 4 h after LPS-treatment, although at reduced expression levels. These results were consistent with those of TNF-α protein level.

DISCUSSION

A biodistribution study of radiolabeled [^{99m}Tc]-LEH in vivo revealed that LEH clearance from circulation is primarily attributable to phagocytic systems of lung and spleen [3]. Several studies have been carried out to investigate the effects of LEH on the functions of phagocytes, including cytokine production, with in vivo and in vitro preparations [4-9]. As in clinical situations where LEH would be administered to patients have a high possibility of underlying infection and/or surgical injury, it is important to clarify whether LEH injection causes or potentiates inflammatory responses such as febrile reactions by modifying the circulatory levels of inflammatory cytokines. TNF-α and IL-6 are regarded as primary indicators in septic shock or postoperational complications [13-15]. In the present study, we evaluated these inflammatory cytokine responses to NRC with or without LPS, using human whole blood as an ex vivo model for studying cytokine responses.

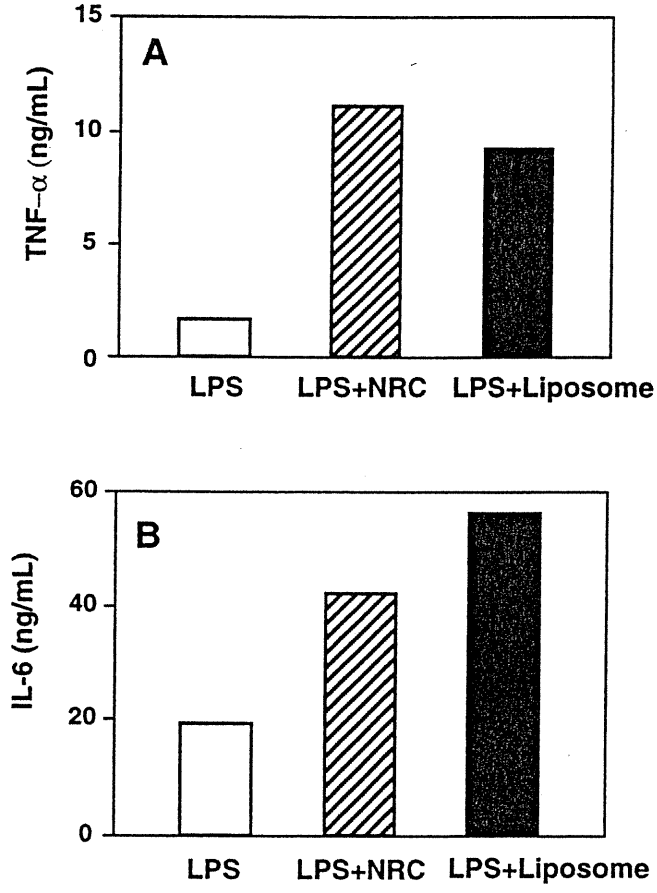

Fig.4 Effects of NRC or liposomes on LPS-induced production of TNF-α (A) and IL-6 (B). Whole blood samples were preincubated with 5% saline, NRC, or liposomes for 24 h and incubated with LPS for a further 24 h. Similar results were obtained in another two experiments.

In the whole blood system, NRC treatment did not cause any induction of TNF-α nor IL-6, and conversely inhibited the constitutive production of these cytokines (Fig. 1). Inhibition of the constitutive TNF-α production by LEH was reported in human peripheral blood monocytes [5] and in the murine-derived monocytic cell line RAW264.7 [8]. However, the decrease in the constitutive IL-6 production by NRC is inconsistent with other reports that intraperitoneal injection of LEH caused a transient increase in serum level of IL-6 in mice [7], and that the mRNA level of IL-6 was elevated by incubation with LEH in the macrophage cell line P388D1 [9]. At

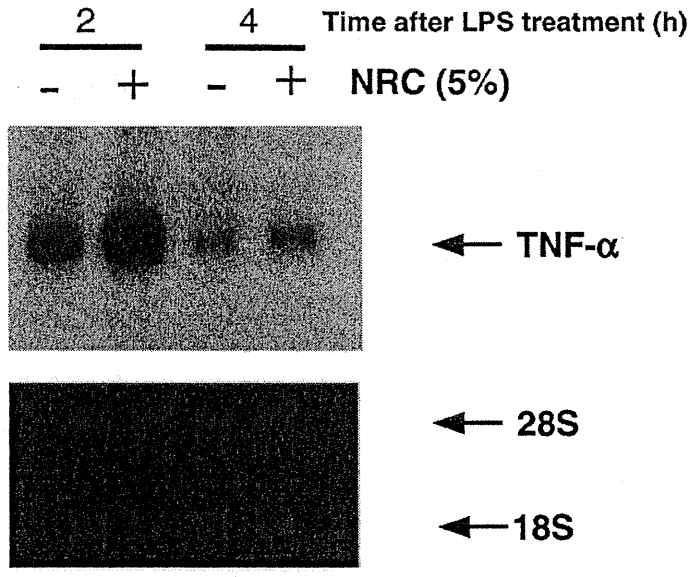

Fig.5 Effects of NRC on LPS-induced expression of TNF-α mRNA. Whole blood samples were preincubated with 5% saline or NRC for 24 h and incubated with LPS for a further 2 or 4 h. Staining of 28S and 18S ribosomal RNAs with ethidium bromide is shown as a loading control.

present, we have no explanation for these opposing results regarding IL-6, but they may be related to differences in species and/or experimental procedures used.

Most of the previous studies evaluating the effects of LEH on cytokine production have utilized LPS to induce cytokine production, while a variety of experimental procedures have been employed. Langdale et al. showed that pretreatment with LEH for 3 h reduced TNF-α protein production elicited by LPS without reduction of TNF-α mRNA level, in cultured rabbit alveolar macrophages [4]. Inhibition of LPS-induced TNF-α production by LEH has also been reported in cultured human monocytes [5] and murine-derived monocytic cell lines [9]. In contrast, it was reported that in vivo liposome pretreatment of rats potentiated on serum TNF-α and IL-6 levels after intraperitoneal LPS challenge, and that Kupffer cells isolated from the liposome-treated rats released more TNF-α and IL-6 after LPS stimulation

[6]. The present results showed that pretreatment of whole blood samples with NRC or empty liposomes markedly potentiated TNF-α production, and to a lesser extent IL-6 production induced by LPS. In addition, northern bloting analysis indicated that the potentiating effect of NRC on LPS-induced production of TNF-α protein is attributable, at least in part, to an increase in TNF-α mRNA level. The potentiation of LPS-induced TNF-α as well as IL-6 production by LEH may lead to modification of the overall severity of the inflammatory response in patients who have underlying infection and/or surgical injury.

As mentioned above, discrepancies among the results of the present and previous studies may be due to several factors, such as experimental procedures, species and/or LEH itself. To our knowledge, this is the first study to have used the human whole blood system to evaluate the effects of LEH on cytokine production. In the whole blood system, multiple blood cell types are capable of responding to LPS, thereby influencing the ultimate cytokine response by potential cellular interactions. Therefore, this system may more accurately reflect the complexity of the in vivo situation than cultures of isolated single cell types. The use of the whole blood system as an ex vivo model would provide further information in regard to the biocompatibility of LEH. However, differences in cytokine responses to LEH under a wide variety of experimental conditions suggests that LEH administration to human subjects may have variable effects on cytokine responses depending upon biological conditions. Further in vivo and in vitro investigations regarding immune responses, including cytokine production must be carried out before LEH clinically can be used.

ACKNOWLEDGMENTS

This work was supported in part by Health Science Research Grant (Artificial Blood Project) from the Ministry of Health and Welfare, Japan.

REFERENCES

1. R.M. Winslow. Hemoglobin-based red cell substitutes: unsolved issues and future directions. In Artificial Red Cells, edited by E. Tsuchida, p117-130 (1995).

2. A.S. Rudolph. Encapsulated hemoglobin: current issues and future goals. Art. Cells. Blood Subs. and Immob. Biotech. 22:347-760 (1994).

3. A.S. Rudolph, R.W. Klipper, B. Goins and W.T. Phillips. In vivo biodistribution of a radiolabeled blood substitutes: 99mTc-labeled liposome-encapsulated hemoglobin in an anesthetized rabbit. Proc. Natl. Acad. Sci. USA 88:10976-10980 (1991).

4. L.A. Langdale, R.V. Maier, L. Wilson, T.H. Pohlman, L.G. Williams and C.L. Rice. Liposome-encapsulated hemoglobin inhibits tumor necrosis factor release from rabbit alveolar macrophages by a posttranscriptional mechanism. J. Leukoc. Biol. 52:679-686 (1992).

5. A.S. Rudolph, R.O. Cliff, B.J. Spargo and H. Spielberg. Transient changes in the mononuclear phagocyte system following administration of the blood substitute liposome-encapsulated haemoglobin. Biomaterials 15:796-804 (1994).

6. P. Bankey, E. Beecherl, D. Bibus. D. See and K. McIntyre. Liposomes modulate Kupffer cell endotoxin response. Arch. Surg. 130:1266-1272 (1995).

7. F.M. Rollwagen, W.C.M. Gafney, N.D. Pacheco, T.A. Davis, T.M. Hickey, T.B. Nielsen and A.S. Rudolph. Multiple responses to administration of liposome-encapsulated hemoglobin (LEH): Effects on hematopoiesis and IL-6 levels. Exp. Hematol. 24:429-436 (1996).

8. A.S. Rudolph, R. Cliff, V. Kwasiborski, L. Neville, F. Abdullah and R. Rabinovici. Liposome-encapsulated hemoglobin modulates lipopolysaccharide-induced tumor necrosis factor-alpha production in mice. Crit. Care Med. 25:460-468 (1997).

9 X.-L. Zhu, W.C.M. Gafney, N.D. Pacheco and F.M. Rollwagen. Kinetics of cytokine gene expression in macrophage and endothelial cell lines following liposome encapsulated haemoglobin (LEH) treatment in vitro. Cytokine 8:541-547 (1996).

10. J.L. Nerad, J.K. Griffiths, J.W.M. Van der Meer, S. Endres, D.D. Poutsiaka, G.T. Keusch, M. Bennish, M.A. Salam, C.A. Dinarello and J.G. Cannon. Interleukin-1β (IL-1β), IL-1 receptor antagonist, and TNF-α production in whole blood. J. Leukoc. Biol. 52:687-692 (1992).

11. M.G. Bouma, T.M.M.A. Jeunhomme, D.L. Boyle, M.A. Dentener, N.N. Voitenok, F.A.J.M. van den Wildenberg and W.A. Buurman. Adenosine inhibits nentrophil degranulation in activated human whole blood. J. Immunol. 158:5400-5408 (1997).

12. J. Szebeni, N.M. Wassef, K.R. Hartman, A.S. Rudolph and C.R. Alving. Complement activation in vitro by the red cell substitute, liposome-encapsulated hemoglobin: Mechanism of activation and inhibition by soluble complement receptor type 1. Transfusion 37:150-159 (1997).

13. H. Bitterman, A. Kinarty, H. Lazarovich and N. Lahat. Acute release of cytokines is proportional to tissue injury induced by surgical trauma and shock in rats. J. Clin. Immunol. 11:184-192 (1991).

14. P. Damas, D. Ledoux, M. Nys, Y. Vrindts, D. De Groote, P. Franchimont and M. Lamy. Cytokine serum level during severe sepsis in human IL-6 as a marker of severity. Ann. Surg. 215:356-362 (1992).

15. Y. Oka, A. Murata, J. Nishijima, T. Yasuda, N. Hiraoka, Y. Ohmachi, K, Kitagawa, T. Yasuda, H. Toda, N. Tanaka and T. Mori. Circulating interleukin 6 as a useful marker for predicting postoperative complications. Cytokine 4:298-304 (1992).

Distribution of Heme Oxygenase Isoforms in Rat Liver

Topographic Basis for Carbon Monoxide-mediated Microvascular Relaxation

Nobuhito Goda,* Kensuke Suzuki,‖ Makoto Naito,‡ Shinji Takeoka,§ Eishun Tsuchida,§ Yuzuru Ishimura,* Takuya Tamatani,‖ and Makoto Suematsu*

*Department of Biochemistry and Department of Obstetrics and Gynecology, School of Medicine, Keio University, Tokyo 160; ‡Second Department of Pathology, Niigata University School of Medicine, Niigata; §Department of Polymer Chemistry, Waseda University, Tokyo; and ‖Pharmaceutical Frontier Research Laboratories, JT Inc. Kanagawa 236, Japan

Abstract

Carbon monoxide (CO) derived from heme oxygenase has recently been shown to play a role in controlling hepatobiliary function, but intrahepatic distribution of the enzyme is unknown. We examined distribution of two kinds of the heme oxygenase isoforms (HO-1 and HO-2) in rat liver immunohistochemically using monoclonal antibodies. The results showed that distribution of the two isoforms had distinct topographic patterns: HO-1, an inducible isoform, was observed only in Kupffer cells, while HO-2, a constitutive form, distributed to parenchymal cells, but not to Kupffer cells. Both isoforms were undetectable in hepatic stellate cells and sinusoidal endothelial cells. Of the two isoforms, HO-2 in the parenchymal cell rather than HO-1 in the Kupffer cell, appears to play a major role in regulation of microvascular tone. In the perfused liver, administration of HbO_2, a CO-trapping reagent that can diffuse across the fenestrated endothelium into the space of Disse, elicited a marked sinusoidal constriction, while administration of a liposome-encapsulated Hb that cannot enter the space had no effect on the microvascular tone. These results suggest that CO evolved by HO-2 in the parenchymal cells, and, released to the extrasinusoidal space, served as the physiological relaxant for hepatic sinusoids. (*J. Clin. Invest.* 1998. 101:604–612.) Key words: heme oxygenase-1 • heme oxygenase-2 • hepatic stellate cells • Kupffer cells• hemoglobin

Introduction

Physiological degradation of heme (iron-protoporphyrin IX) into biliverdin, iron, and carbon monoxide (CO)[1], is mediated by heme oxygenase (HO, EC1.14.99.3) which consists of two distinct isoenzymes called HO-1 (1) and HO-2 (2). HO-1, also known as the heat shock protein-32, is induced by a variety of stressors such as hyperthermia (3), cytokines (4), and intake of heavy metals (5). This isoform is considered to be present in spleen, a major organ for destruction of senescent erythrocytes, and in liver stimulated with endotoxin (6) or ischemia reperfusion (7). On the other hand, HO-2 is a constitutive form known to be abundant in brain, testis, and unstimulated liver of rodents and humans as reported previously (8).

Recently, several lines of evidence have indicated that the heme oxygenase reaction serves as a key mechanism to maintain the integrity of physiological function of organs such as liver through the action of the reaction products CO and bilirubin. We have shown that in the perfused rat liver, zinc protoporphyrin IX (ZnPP), a heme oxygenase inhibitor, elicits a marked increase in the vascular resistance as a consequence of sinusoidal constriction (9, 10). Furthermore, the ZnPP administration turned out to induce bile acid–dependent choleresis that coincided with depletion of the venous CO flux and biliary excretion of bilirubin, another product of heme degradation (11). Therefore, the results have suggested that CO generated by heme oxygenase serves as a regulator of hepatobiliary functions under physiological conditions. On the other hand, bilirubin scavenges various oxidants such as hydroxyl radical and singlet oxygen, and is thus considered an endogenous antioxidant that protects cells from oxidative insults (12, 13).

In an attempt to understand the aforementioned roles of heme oxygenase, we investigated the intrahepatic distribution of HO-1 and HO-2 using newly developed mAbs against these isozymes. The results indicated distinct distribution patterns of these isozymes among the liver cells, and thus provided a microtopographic basis for the mechanism of CO-mediated sinusoidal relaxation.

Methods

Animals. Male Wistar rats (260–300 g) were obtained from Saitama Animal Laboratory (Saitama, Japan). Female BALB/c (6–10 wk old) and CRJ; CD-1nu mice (7 wk old) were purchased from Charles River Japan Inc. (Atsugi, Japan). All animals were allowed free access to laboratory chow and tap water. Rats were anesthetized intraperitoneally with pentobarbital sodium (50 mg/kg), and the liver, spleen, and testis were then excised to collect samples for Western blotting analysis and immunohistochemistry. In separate sets of experiments, rats were pretreated with intraperitoneal injection of LPS (O-111B4, 4 mg/kg) 6 h before the sample collection.

Transformant cells expressing HO-1 and -2. Rat hepatocytes were isolated and cultured according to the previous method (14). Total cellular RNAs were extracted using ISOGEN (Nippon Gene, Tokyo, Japan) from the cells pretreated with or without heat treatment for 4 h at 42°C. The first-strand cDNAs were synthesized with the mixture of oligo $(dT)_{20}$ primers and random hexamers $(pd[N]_6)$ using reverse transcriptase. PCR primers (rHO-1: 5′-d[GCC TGA ACT AGC

Address correspondence to Associate Professor Makoto Suematsu, M.D., Ph.D., Department of Biochemistry, School of Medicine, Keio University, 35 Shinanomachi, Shinjuku-ku, Tokyo 160, Japan. Phone: +8-3355-2827; FAX: +81-3-3358-8138; E-mail: msuem@mc.med.keio.ac.jp

Received for publication 28 July 1997 and accepted in revised form 5 December 1997.

1. *Abbreviations used in this paper:* CO, carbon monoxide; HO, heme oxygenase; HRP, horseradish peroxidase; rHO, rat heme oxygenase; ZnPP, zinc protoporphyrin IX.

J. Clin. Invest.

0021-9738/98/02/0604/09 $2.00
Volume 101, Number 3, February 1998, 604–612
http://www.jci.org

CCA ATT GCG CGA TGG AGC GC]-3′, 5′-d[CTC TGG GGG CCA AGT CGA CAT TTA CAT GGC AT]-3′; rHO-2: 5′-d[AGG GCA GCA CAA AGA ATT CAG CAA CAA ATG TCT]-3′, 5′-d[ATG CAA ACA ACA TGT CGA CTC CTT CAC ATG TA]-3′) were synthesized based on the nucleotide sequences of rat HO-1 (rHO-1) and -2(rHO-2) reported by Shibahara et al. (1) and Rotenberg and Maines (15). Using these primers, rHO-1 and -2 were amplified from first-strand cDNAs based on the PCR using AmpliWax PCR Gem 100 (Takara Biomedicals, Tokyo, Japan). The pEFneo plasmid vector containing the EF-1a promoter was used to express rHO-1 and -2 (16). An adaptor was attached to the Sal I site at the 3′ end of both PCR products, resulting in construction of the Not I site which was present in multiple cloning sites of the pEFneo plasmid vector. The resulting PCR products were sequenced to confirm their identities, and were named pEFneo-rHO-1 and pEFneo-rHO-2, respectively. The expression plasmid DNAs, pEFneo-rHO-1 and -2, were transfected into WR19L cells (mouse T cell line) by electroporation (17). The transfected cells, designed as WR19L-rHO-1 and -HO-2, were cultured in RPMI 1640 supplemented with 10% FCS under 5% CO_2. After the 24-h incubation, geneticin (Gibco-BRL, Gaithersburg, MD) was added to the culture medium at a final concentration of 0.9 mg/ml to obtain stable transformants.

HO activities in the transformants. Heme oxygenase activities in transformants were determined by measuring bilirubin formation. The cells were harvested and washed twice with PBS at pH 7.0. To remove insoluble fraction, the cells were lysed in 4 volumes of 1% nonidet P-40 solution containing 150 mM NaCl, phenylmethylsulfonyl fluoride (1 mM), and 50 mM Tris HCl (pH 8.0) for 30 min on ice. The supernatants were collected by centrifugation at 10,000 *g* for 15 min. The reaction mixture contained the following in a final volume of 300 μl: glucose 6-phosphate (1 mM), glucose 6-phosphate dehydrogenase (0.167 U/ml), NADP (0.8 mM), hemin (15 μM), $MgCl_2$ (2 mM), NADPH-cytochrome P450 reductase (0.01 mg/ml; Gentest, Woburn, MA), rat liver cytosol (3.3 mg protein/ml), potassium phosphate buffer (27 mM, pH 7.4), and the supernatant from the transformant cells. Incubation was carried out at 37°C for 30 min. An equal volume of chloroform was added to the reaction mixture to stop the reaction, and bilirubin generated was extracted into the chloroform fraction. After centrifugation at 10,000 *g* for 15 min, amounts of bilirubin in the chloroform extract was examined as previously reported by Yoshida and Kikuchi (18).

Hybridomas producing the mAbs against rat heme oxygenase isoforms. The foot pads of 6-wk-old female BALB/c mice were injected every week with 1 mg protein of the microsomal fraction obtained from WR19L-rHO-1 and -HO-2, emulsified the first time with Freund's complete adjuvant, and the rest with the incomplete adjuvant. The immunization was repeated 5–10 times. 48 h after the last immunization, bilateral inguinal and parietal abdominal lymph nodes of immunized mice were harvested, and B lymphocytes were fused with mouse myeloma PAI cells in the ratio of 1:3–5 in 50% polyethylene glycol 4000 (Boehringer Mannheim, Mannheim, Germany). Hybridomas were cultured in ASF104 medium (Ajinomoto, Tokyo, Japan) containing 10% FCS and HAT (hypoxanthine, aminopterin, and thymidine) medium for 2 wk.

Selection of hybridomas producing mAbs against rHO-1 and -2 was carried out by examining the specific immunoreactivity of the supernatant fraction of their culture medium with membrane-permeabilized WR19L cells that expressed rHO-1 and -2, respectively. To this end, WR19L cells expressed rHO-1 and their wild-type was collected and fixed with 2% paraformaldehyde for 10 min at 4°C in PBS at pH 7.4. These cells were washed twice with PBS, and were blocked for 20 min at 4°C in RPMI 1640 supplemented with 10% FCS. The cells were then incubated with the supernatants of the hybridomas and 0.5% saponine in the same plates for 30 min at 4°C. After washing twice with PBS, these cells were further incubated with sheep anti–mouse $F(ab')_2$ fragments of IgG conjugated with fluorescein (Organan-Teknika-Cappel, Durham, NC) for 30 min at 4°C. After the rinse with PBS, the cells served as samples for the analysis using an EPICS flow cytometer (Coulter Electronics, Hialeah, FL). To obtain a single clone specifically producing the desired mAb, subcloning of the hybridomas was further carried out by dilution of the cell number. A similar protocol was applied to screen the hybridomas that generated anti-rHO-2 mAbs. Finally, the anti-rHO-1 and -2 mAbs used in this study were named GTS-1 and GTS-2, respectively.

Purification and isotyping of monoclonal antibodies. Ascites were elicited in 8-wk-old female CRJ; CD-1nu mice that were pretreated with 2, 6, 10, 14-tetramethyl pentadecane by intraperitoneal injection of a desired hybridoma at a dose of 2×10^6 cells/mouse. The ascitic fluid was collected, and the mAbs were purified by sequential precipitation with caprylic acid and 45% ammonium sulfate as previously described (19). The purity of the mAbs was assessed by SDS-PAGE. The subclasses of purified mAbs were determined by a mouse monoclonal isotyping kit (RPN 29; Amersham International, Little Chalfont, UK).

Western blot analysis. Microsomal fractions isolated from spleen, liver, and testis of rats were subjected to Western blot analyses. Soluble fractions derived from stable transformant cells pretreated with 1% Nonidet P-40 solution served as the positive control samples. After denaturing, these proteins were subjected to 10% SDS-PAGE and then transferred to an Immobilon polyvinylidene difluoride transfer membrane (Daiichi Pure Chemicals, Tokyo, Japan). The membrane was blocked with Block-Ace (Dainippon Pharm. Co., Osaka, Japan) for at least for 3 h, and was followed by incubation with either GTS-1 or GTS-2 at 1 μg/ml overnight at 4°C. After washing with PBS containing 0.1% Tween 20, the membrane was immersed in a biotinylated anti–mouse IgG $F(ab')_2$ fragment (RPN 1061; Amersham International) diluted in PBS containing 1%BSA. The samples were then treated with avidin and horseradish peroxidase (HRP)-conjugated biotin according to manufacturer's protocol (Vectastain Elite ABC kit; Vector Laboratories, Inc., Burlingame, CA). Chemiluminescence associated with the antigen-specific HRP reaction was visualized by the Molecular Imager (GS-525, Nippon Bio-Rad. Co., Tokyo, Japan) and the ECL detection kit (Amersham International). The Western blot analysis was repeated to confirm reproducibility using the samples collected from at least three individual rats.

Immunohistochemistry. Rat spleen, liver, and testis were fixed for 4 h at 4°C in periodate-lysine-paraformaldehyde solution. The samples were washed sequentially for 4 h with PBS containing 10, 15, and 20% sucrose, and were embedded in OCT compound (Miles Laboratories, Elkhart, IN). In some experiments, fresh-frozen sections from these organs were prepared and fixed with acetone. The sections (10-μm thickness) were treated with normal horse serum to minimize nonspecific staining. These tissues were incubated with mAbs GTS-1 or GTS-2 dissolved in 1% BSA/PBS at a final concentration of 1 μg/ml for at least 2 h at 25°C or overnight at 4°C. After several washes with PBS, the sections were stained with biotinylated anti–mouse IgG for 1 h (Vectastain Elite ABC kit; Vector Laboratories, Inc.). To prevent endogenous peroxidase reactions, the samples were pretreated with 0.3% H_2O_2 in cold methanol for 30 min, and were subsequently incubated with avidin and HRP-conjugated biotin for 30 min. Finally, 0.1 mg/ml of 3, 3′-diaminobenzidine (DAB) tetrahydrochloride were applied to sections for 5 min. The sections were counterstained with methyl green after fixation with 20% formaldehyde for 20 min, and slides were coverslipped with aqueous mounting medium. To confirm the specificity of immunohistochemical localization by the antibodies, the antibodies preabsorbed with an excess of adequate antigens in advance were used. In separate sets of experiments, sections of the liver were double-stained by a method using DAB and nickel chloride to identify different types of nonparenchymal cells (20). To this end, anti–rat macrophage mAb Ki-M2R (BMA Biomedicals Ltd., Augst, Switzerland) and antidesmin II mAb (Bio-Science Products AG, Emmenbrucke, Switzerland) were used to stain Kupffer cells and hepatic stellate cells, respectively. By these protocols, cells reacting only with the initial primary Ab (GTS-1 or -2) stained light brown, while those reacting with the second primary Ab stained bright purple. When reacting simultaneously with both primary Abs, the cells were identified as those stained dark purple.

Isolated perfused liver preparation. The livers of male Wistar rats were excised and perfused with Hb-free and albumin-free Krebs Ringer solution (pH 7.4, 37°C) gassed with carbogen (95% O_2, 5% CO_2) according to our methods described previously (10, 21). The perfusate contained 30 μM sodium taurocholate, and was pumped through the liver at a constant flow rate of 4.0 ml/min/g liver. The preparation allowed us to examine the vasoactive responses in sinusoids while simultaneously monitoring the whole organ vascular resistance, as described elsewhere (10, 11).

Determination of CO generated by isolated cultured hepatocytes. Primary cultured rat hepatocytes were prepared by digesting the liver with type IV collagenase (Wako Pure Chemical Industries, Ltd., Osaka, Japan) according to the previous method (14). To estimate the rate of heme degradation in the isolated cultured hepatocytes, concentrations of CO were determined in the culture medium. To this end, the hepatocyte suspension (5×10^6 cells/ml) was incubated in a specially arranged double-lumen bioreactor as described previously (mini PERM; Heraeus Instruments, Inc., Hatz, Germany; 22). 2 ml of the culture medium was collected 2 h after the start of culture, and was used as a sample to determine CO. CO in the sample medium was determined by Mb-assisted spectrophotometry as described elsewhere (10).

Preparation of Hb and liposome-encapsulated Hb. To examine the role of endogenously generated CO in regulating the steady-state vascular tone in the liver, free and liposome-encapsulated Hbs, hereafter designated as free Hb and HbV, respectively, were used as a tool to trap CO in and around the sinusoidal space. Free Hb, HbV, and met Hb, a control tool that can scavenge NO but not CO, were prepared using outdated human erythrocytes as described previously (23, 24). The distribution of the diameter of the HbV was measured by a light-scattering particle analyzer (Submicron Particle Analyzer N4-SD; Coulter). The mean value of the diameter of HbV used in this study was ~250 nm. Previous histochemical studies (25) revealed that when administered into the systemic circulation, HbV with this size diameter was partly captured in tissue macrophages including Kupffer cells, but did not enter the hepatic parenchyma. On the other hand, free Hb was readily trapped by the parenchymal cells because of the presence of fenestration in sinusoidal endothelium, the diameter of which ranges from 100 to 150 nm (26, 27). Both free Hb and HbV were used for experiments within 10 d after completing the preparation procedures. These samples were added in the perfusate at 1.5 g/dl in Hb concentrations, the value equivalent to ~10% of the physiological concentration in rat blood samples.

Microangiography of sinusoids in perfused liver. To examine whether free Hb and HbV alter the diameter of sinusoids by an unknown mechanism, digital microangiography in the perfused liver preparation was carried out as described previously (10, 28). To obtain a quality of the microvascular images, real-time laser confocal imaging system was applied to intravital microscopy according to our recent method (29). The surface of the perfused liver was observed through an inverted-type intravital microscope assisted by a line-scan laser confocal imager (Insight/IMD300; Meridian Instrs., Inc., Okemos, MI) and the hepatic microcirculation was visualized by a silicon intensified target imaging camera (C2400-08; Hamamatsu Photonics, Hamamatsu City, Japan). To visualize the hepatic sinusoidal vessels, 100 μl of 1% FITC-dextran solution was injected transportally every 5 min after the start of experiments, and the microvasculature was visualized by epi-illuminating at 488 nm using an argon laser light source. This system also allowed us to examine the topographic relationship between the sites of sinusoidal constriction and those of hepatic stellate cells, the liver-specific pericytes, by visualizing their vitamin A autofluorescence under epi-illuminating at 360 nm (10, 30). Imaging of vitamin A–associated autofluorescence was carried out right before the start of FITC–dextran transportal injection. Recording intrahepatic vitamin A autofluorescence also helped us to examine whether the FITC-dextran–assisted microangiography was carried out at identical depths of focus among a series of microfluorographs taken at different times: When topographic patterns of the hepatic stellate cells in a field of interest were different among the images recorded in the same preparation, a series of FITC dextran assisted microvascular images were discarded from the data analysis for measurements of sinusoidal diameters. The microangiographs were digitally processed, and were used for morphometrical analysis of the diameter changes as described previously (10). In brief, measurements of the diameter were carried out every 10 μm along the longitudinal axis of sinusoids from the most efferent sites adjacent to central venules to the afferent sites. This procedure gave ~20–30 measurements for each sinusoid. At least 15 sinusoids were evaluated in a single experiment.

Results

Monoclonal antibodies against rat heme oxygenase. To verify immunoreactive specificity of mAbs against rHO-1 (GTS-1) and -2 (GTS-2), flow cytometry and Western blotting analysis were carried out using the stable transformants that expressed rHO-1 or -2 proteins as described in Methods. As shown in Fig. 1 *A*, GTS-1 stained WR19L-rHO-1 cells positively, while it stained neither mock-transfected WR19L cells nor WR19L-rHO-2 cells. On the other hand, WR19L-rHO-2 cells exhibited a positive immunostaining by GTS-2, whereas the mock-transfected cells and the WR19L-rHO-1 cells displayed negative staining, indicating a paucity of cross-reaction between the two mAbs as to recognition of the heme oxygenase isoforms. These findings were confirmed by Western blotting analysis (Fig. 1 *B*): GTS-1 and GTS-2 exhibited their specific immunoreactivities to rHO-1 and -2 on molecular sizes of 32 kD and

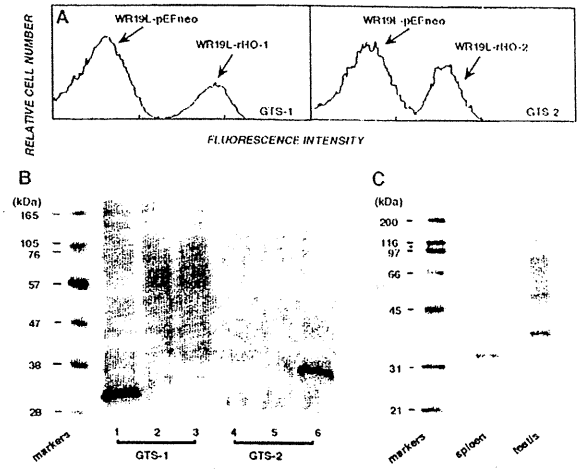

Figure 1. Characterization of newly developed monoclonal antibodies against rat HO isoforms. (*A*) Flow cytometric analysis to examine specific binding of mAbs GTS-1 and -2 to WR19L cells expressing rHO-1 and rHO-2, respectively. (*B*) Western blotting analysis showing the specific binding of mAbs GTS-1 and -2 to cell lysates extracted from the stable transformants WR19L-rHO-1 and WR19L-rHO-2. Lanes *1* and *4*, WR19L-rHO-1; lanes *2* and *5*, WR19L-pEFneo; lanes *3* and *6*, WR19L-rHO-2. Note that GTS-1 and -2 specifically recognize single bands at 32 kD and 36 kD, respectively. (*C*)Western blotting analysis showing the binding of mAbs GTS-1 and -2 to microsomal fractions (10 μg per lane) isolated from rat spleen and testis, respectively. Note the preferential expression of HO-1 in spleen and HO-2 in testis.